MiR-519a/522-5p from pancreatic cancer-secreted exosomes promotes tumor invasion by enhancing Warburg effect

Qi Ling (lingqi@zju.edu.cn)
Zhejiang University School of Medicine
Shi Feng
Zhejiang University School of Medicine
Ruihan Chen
Zhejiang University School of Medicine
Haitao Huang
Zhejiang University School of Medicine
Yimou Lin
Zhejiang University School of Medicine
Jingyu Jiang
Zhejiang University School of Medicine
Jinlong Cui
Zhejiang University School of Medicine
Tingbo Liang
Zhejiang University School of Medicine

Research Article

Keywords: Pancreatic ductal adenocarcinoma, Exosome, Biomarker, miR-519a/522-5p, Warburg effect

Posted Date: April 28th, 2022

DOI: https://doi.org/10.21203/rs.3.rs-1540878/v2

Abstract

Background: Pancreatic ductal adenocarcinoma (PDAC) is a highly aggressive malignancy with poor prognosis. Exploring novel serum biomarkers and the underlying mechanism is crucial for the early diagnosis and precise therapy of PDAC.

Methods: Exosomes were isolated from serum samples of 92 PDAC patients and 44 healthy subjects. Serum exosomal microRNAs (exo-miRNAs) were detected by small RNA sequencing, verified by qRT-PCR, and their diagnostic performance and prognostic value were evaluated. *In vitro* experiments and orthotopic tumor mouse models were conducted to investigate the effect of miR-519a/522-5p on PDAC. Integrated transcriptomics and metabolomics were used to explore the underlying mechanism of miR-519a/522-5p.

Results: Compared to the healthy control, all three PDAC subgroups (stage I-III) displayed a specific deregulated serum exo-miRNA profile. A panel of 3 serum exo-miRNAs (let-7g-3p, miR-490-5p, and miR-519a/522-5p) was established as novel diagnostic biomarkers for PDAC, which exhibited high sensitivity and specificity in clinical cohort. Among the three exo-miRNAs, miR-519a/522-5p was found to be an independent prognostic factor for PDAC and associated with tumor features particularly invasion/metastasis. *In vitro* and *in vivo* experiment confirmed that miR-519a/522-5p promoted invasiveness/metastasis of PDAC cells. Moreover, miR-519a/522-5p could be effectively delivered via exosomes and increased the invasiveness of recipient PDAC cells. Multi-omics analysis showed a comprehensive miR-519a/522-5p-regulated molecular network, in which glycolysis played a central role. We further validated that miR-519a/522-5p enhanced glycolysis by targeting sestrin2.

Conclusion: Serum exo-miRNAs could be novel and promising candidates for precise diagnosis and treatment of PDAC. Tumor-derived exo-miR-519a/522-5p promotes PDAC cellular invasiveness by enhancing Warburg effect.

Background

Pancreatic ductal adenocarcinoma (PDAC) is a highly lethal malignancy with an increasing mortality during the past decades [1]. Surgical resection remains the only hope for PDAC patients to achieve a potential long-term survival. However, only 15–20% of PDAC patients initially diagnosed at early stage and treated with radically surgery [2]. The majority of PDAC patients are diagnosed at late stage with a median survival time of 3–14 months, even treated with the newly developed therapies, such as PD-1/PD-L1 antibody [3]. Therefore, effective early diagnosis and screening is a key strategy in improving the prognosis of PDAC patients.

Serum biomarkers are of help in screening and early diagnosis of PDAC. Since the carbohydrate antigen 19 – 9 (CA19-9) was identified in 1980, it became the most widely used biomarker of PDAC in clinical practice. However, the sensitivity and specificity of serum CA19-9 in the diagnosis of early stage PDAC were insignificant, only 55.6–75.0% and 56.0–81.5% [4]. In recent years, new biomarkers are developing

to better understand the molecular mechanisms of carcinogenesis and progression of PDAC. Exosomes or extracellular vesicles have been considered as one of the most promising tumor biomarker and therapeutic target.

Exosomes are small endosomal-derived vesicles with diameters ranging from 30–200 nm, which carry proteins, lipids, miRNAs, lncRNAs, and circRNAs and play an important role in cell-to-cell communication via their cargo [5]. In blood, cancer-secreted exo-miRNAs occurred earlier than cell-free nucleic acid caused by necrosis. Additionally, exo-miRNAs are protected from degradation by endogenous RNase, hence they are more stable compared with the circulating miRNAs [6]. Recent studied suggested exo-miRNAs as ideal diagnostic and prognostic biomarkers in PDAC patients. Madhavan et al. [7] found that miR-1246, miR-4644, miR-3976 and miR-4306 were significantly upregulated in 83% of serum-exosomes in PDAC patients, which had a sensitivity of 81% and a specificity of 94% for the diagnosis of PDAC. In another study, low level of exo-miR-19b was found to be superior to CA19-9 for the diagnosis of PDAC [8]. Furthermore, plasma exo-miR-451a showed a significant correlation with tumor size and stage and could be a valid biomarker for the prediction of tumor recurrence in PDAC patients [9]. Besides, experimental studies demonstrated that exo-miRNAs played key roles in tumor invasion, angiogenesis and immune response. For instance, exo-miR-301a promoted PDAC metastasis by mediating M2 macrophage polarization via PTEN/PI3Kγ pathway [10], while exo-miR-98-5p inhibited PDAC proliferation and metastasis by targeting MAP4K4 [11].

In this study, we compared the serum exo-miRNA profiles between patients with different PDAC stages and health controls. We found a common PDAC-specific exo-miRNA panel in different tumor stages and identified three serum exo-miRNAs (miR-490-5p, let-7g-3p, miR-519a/522-5p) as diagnostic biomarkers in the validation cohort. Moreover, we demonstrated that exo-miR-519a/522-5p was an independent prognostic factor and closely associated with tumor characteristics. Further *in vitro* and *in vivo* experiments indicated that miR-519a/522-5p enhanced invasiveness/metastasis of PDAC cells and could be effectively transported by exosomes. Combined transcriptomics and metabolomics analyses revealed that miR-519a/522-5p drove metabolic reprogramming particularly glycolysis in PDAC cells possibly through directly targeting sestrin2 (SESN2), a pivotal protein in glucose metabolism.

Materials And Methods

PDAC patients and clinical samples

Ninety-two PDAC patients (histological verified) and 44 healthy subjects between June 2017 and October 2019 were enrolled from the First Affiliated Hospital, Zhejiang University School of Medicine. Patients were excluded if they had undergone radiotherapy or chemotherapy, a previous history of other types of cancer, or acute pancreatitis when the study was initiated. All participants' blood samples were taken before treatment. We also collected 32 pairs of fresh frozen PDAC tissues and adjacent non-cancerous tissue. All tumors were histologically staged, according to AJCC-TNM (American Joint Committee on Cancer; tumor, node, metastasis) classification 2018. Additionally, we followed 92 PDAC patients over a

2-year period. This study was approved by Ethics Committee of hospital, and written informed consent was obtained from all patients.

Isolation and characterization of exosomes from the serum

A total of 2 mL of serum was mixed with RiboTM Exosome Isolation. Reagent and exosome isolation were performed according to the manufacturer's instructions (miRCURY Exosome Serum/Plasma Kit, Qiagen, Hilden, Germany, Cat. Number: 76603). The presence of exosomes was identified as described previously [12].

Next-generation small RNA sequencing

Purified serum exosomal RNAs were ligated with 3'RNA adapter and followed by 5'adapter ligation. Subsequently, the adapter-ligated RNAs were subjected to RT-PCR and amplified with a low-cycle. Then the PCR products were size selected by PAGE gel according to instructions of NEBNext® Multiplex Small RNA Library Prep Set for Illumina® (Illumina, USA). The purified library products were evaluated using the Agilent 2200 TapeStation and diluted to10 pM for cluster generation in situ on the HiSeq2500single-end flow cell followed by sequencing (1 × 50 bp) on HiSeq 2500.

Quantitative Real-Time Reverse Transcription Polymerase Chain Reaction (qRT-PCR

qRT-PCR was performed as described previously [12]. All miRNA sequences and primers sequences used for qRT-PCR were listed in Table S1-S3.

Cell culture and transfection

The human PDAC cell lines PANC-1 (Catalog number SCSP-535), BxPC-3 (Catalog number TCHu012), AsPC-1 (Catalog number TCHu 8), CFPAC-1 (Catalog number TCHu112) and MIA PaCa-2 (Catalog number SCSP-568) were purchased from the Type Culture Collection of the Chinese Academy of Sciences (Shanghai, China). Normal pancreatic cell CCC-HPE-2 was purchased from the China Infrastructure of Cell Line Resource (Beijing, China). All cells were maintained in a humidified atmosphere containing 5 % CO_2 at 37 °C. Cell transfection was performed as described previously [12]. Sequences of miR519a/522-5p mimics and inhibitor were listed in Table S4.

Cellular functional experiments

Cellular functional experiments were performed as described previously [12, 13]. Cell Counting Kit-8 (CCK-8) kit (RiboBio, Guangzhou, China) was utilized to evaluate the proliferation of the cells. The Transwell system (Corning Inc.) was used for the PDAC cells invasion assay. Apoptosis analysis was conducted to assess cell apoptosis. The experiments were repeated three times with triplicates.

Tumor xenograft model *in vivo*

A lentiviral vector system (Genepharma, Shanghai, China) as described previously was constructed for stable expression of miR-519a/522-5p in PANC-1 cells [12]. The *in vivo* experiment was approved by the Ethical Committee of hospital. The Balb/c nude mice (6-8 weeks) were purchased from Shanghai Experimental Animal Center, Chinese Academy of Science, and randomly divided into 2 groups (n = 7). Mice were anesthetized by isoflurane inhalation, and the pancreas was exposed via an abdominal incision. Injected with 1×10^7 miR-519a/522-5p-overexpressing or empty transduced PANC-1 cells (50 μL in PBS) into the head of pancreas. Then the abdomen was closed. After six weeks, luciferase imaging system was applied to evaluate the metastasis of tumors and then all mice were euthanized for autopsy.

miR-519a/522-5p transportation detection

We performed co-culture experiment to detect the manner of miR-519a/522-5p intercellular delivery as described previously [12].

Exosome electroporation transfection

For further improving the transfection efficiency, miR-519a/522-5p or Cy3-miR-519a/522-5p mimics were encapsulated into the exosomes via electroporation. 60 μg exosomes and 300 pmol miRNA mimics were mixed in 400 μL electroporation buffer. The exosomes were electro transfected at 250 V using bio-rad electroporation apparatus (Hercules, CA, USA). The electroporation efficiency was assessed by qRT-PCR.

Transcriptomics and Metabolomics

Transcriptome sequencing and liquid chromatographymass spectrometry (LC-MS) analysis were carried out as described previously [14]. Kyoto Encyclopedia of Genes and Genomes (KEGG) analysis of differentially expressed genes and metabolites were performed with the cluster Profiler R package.

Measurement of extracellular acidification rate

The Glycolysis Stress Test Kit (Seahorse Bioscience, Billerica, MA, USA) was used to determine glycolytic capacity on the Seahorse XFe96 Extracellular Flux Analyzer (Seahorse Bioscience, USA) according to the manufacturer's instructions. Briefly, PANC-1 and BxPC-3 cells transfected with miR-519/522-5p mimics/NC and inhibitor/inhibitor-NC were seeded in a XF96-well plate at a density of 1×10^5 per well and incubated overnight. Then washing the cells with Seahorse buffer. For extracellular acidification rate (ECAR) assessment, cells were injected with 10 mM glucose, 1 μM oligomycin, and 80 mM 2-deoxy-glucose (2-DG) to measure the ECAR.

Luciferase reporter assay

Luciferase reporter assay was performed as described previously [12]. Briefly, the dual-luciferase vectors of SESN2 and the mutants of binding sites of SESN2 to the miR-519a/522-5p were constructed separately: pmirGLO-SESN2-wild type (wt) and pmirGLO-SESN2-mutation (mut). Firefly and Renilla

luciferase activities were measured using the Dual-Luciferase Reporter Assay kit (Promega, Madison, USA).

Statistical analysis

GraphPad Prism 8.0 Software (GraphPad Software, La Jolla, CA, USA) and SPSS 22.0 statistical software (IBM Corp. Armonk, NY, USA) were used to perform the statistical analyses. The experimental data were expressed as mean ± standard deviation (SD). The comparison between two groups was performed using Student's t-test if the data followed a normal distribution; otherwise, the nonparametric Mann-Whitney test was used. One-way analysis of variance was employed for comparison among more than two groups, followed by Tukey's post-hoc test. Receiver operating characteristic curve (ROC) was used to assess the sensitivity, specificity, and respective areas under the curve (AUC) and its 95% of confidence interval (CI). Univariate and multivariable logistic regression models were applied to test the performance of single biomarkers and biomarker combinations in differentiating PDAC from control samples. MedCalc Statistical Software 14.10 (MedCalc Software, Ostend, Belgium) was used to determine the cut-off points and compare AUC of miRNAs and CA19-9. The risk factors of PDAC prognosis were screened with the univariate (the log-rank test) and multivariate (the stepwise Cox multivariate proportional hazard regression model) analysis. The overall survival and recurrence-free survival between PDAC patient with high or low expression of miRNAs were computed using the Kaplan–Meier method and the log-rank test was used to assess statistical significance. The correlation between clinicopathological characteristics and serum exo-miR-519a/522 expression was evaluated by a χ^2 test. Statistical significance was assumed at $P < 0.05$.

Results

Patient characteristics

A total of 92 PDAC patients were included. Patient characteristics and tumor features are shown in Table S5. All patients were treatment-naive before enrollment. Eighty patients received surgery including 7 with liver metastasis. Adjuvant therapy including chemotherapy and radiotherapy were performed in 77.5% (62/80) patients receiving surgery. The 1- and 3-yr recurrence-free survival was 52.8% and 14.5%, respectively. The 1- and 3-yr patient overall survival was 59.7% and 15.9%, respectively.

Serum exo-miRNA profiles of PDAC

We stratified PDAC patients into early stage PDAC group (stage I-IIA), lymph node metastatic PDAC group (stage IIB-III) and liver metastatic PDAC group (stage IV). We collected serum samples from 12 PDAC patients (4 from each subgroup) and 4 healthy subjects to detect the exo-miRNAs using a sequencing. We compared the serum exo-miRNA profiles between different PDAC subgroups and control group (Table S6). We observed that all 3 PDAC subgroups displayed 2 significantly up-regulated miRNAs and 9 down-regulated miRNAs using a selection criteria of fold change > 2, $P < 0.05$ and the largest rank sum differences (Fig. 1A). Interestingly, we noted that among the 9 down-regulated miRNAs, 8 belonged to

chromosome 19 microRNA cluster (C19MC) and 6 shared the same sequence (www.mirbase.org). In addition, miR-519a-5p and miR-522-5p were found to be located at the shortest subset of C19MC (length of 1270bp) named as miR-519a/522-5p.

To verify the results, we enrolled the remaining 80 PDAC patients and 40 age- (± 5 yr) and gender-matched controls (2:1). There was no significant difference in co-morbidities including hypertension, diabetes, and dyslipidemia between PDAC patients and control subjects (Table S7). We detected the PDAC-associated serum exo-miRNAs from the two groups using qRT-PCR. Finally, significantly increased serum exo-let-7g-3p and miR-490-5p and decreased miR-519a/522-5p were found in PDAC group as compared to the control group (Fig. 1B). Whereas the expression of other miRNAs had no significant differences (Fig. S1A).

Serum exo-miRNAs as biomarkers in the diagnosis of PDAC

To evaluate the diagnostic performance of the above 3 serum exo-miRNAs, we performed AUC analysis and observed that all 3 miRNAs showed AUCs > 0.75 for distinguishing 80 PDAC patients from 40 controls. There was no significant difference between the 3 miRNAs and the typical biomarker CA19-9. In contrast, CEA presented the lowest AUC (all $P < 0.05$, Fig. 1C).

To further establish a valid serum biomarker panel, we randomly (1:1) divided the cohort into a training set and a validation set. We next selected the cut-off value of serum exo-miRNAs by considering both diagnostic sensitivity and specificity. CA19-9 positive (> 37 U/mL) rate was 70% (28/40) in PDAC patients. We then established biomarker panels by integrating serum exo-miRNAs with CA19-9 in the training group. The panels displayed significantly enlarged AUCs in the diagnosis of PDAC than CA19-9 alone in both training and validation sets (Fig. 1D). The diagnostic sensitivity, specificity and accuracy are shown in Table S8. Approximate 70% of PDAC patients with negative CA19-9 could be diagnosed via the supplement of each of the 3 exo-miRNAs. Moreover, the diagnostic accuracy would be perfect after the combination of CA19-9 and all 3 exo-miRNAs with an AUC value of 0.99.

Serum exo-miR-519a/522-5p is associated with patient prognosis and tumor features

Survival analysis were conducted to assess the prognostic value of serum exo-miRNAs. We observed that miR-519a/522-5p could differentiate patients with high and low recurrence/death risk (Fig. 1E), whereas let-7g-3p and miR-490-5p could not (Fig. S1B). In univariate COX hazard analysis, AJCC stage III-IV, histological grade G3, vessel invasion, lymph node metastasis, liver metastasis and low expression of serum exo-miR-519a/522-5p were the risk factors for tumor recurrence and patient death (Table S9). In multivariate analysis, serum exo-miR-519a/522-5p was found to be the independent factor for both tumor recurrence and patient death (Fig. 1F).

We next analyzed the correlations between the expression of serum exo-miR-519a/522-5p and tumor features. There was a significant positive correlation between low serum exo-miR-519a/522-3p

expression and lymph node/liver metastasis, neural invasion, adjacent tissue invasion, and histological grade G3 (Table S10).

Low miR-519a/522-5p level in serum exosomes links to the accumulation of miR-519a/522-3p in cancer

We detected the expression of miR-519a/522-5p in PDAC tissue and paired adjacent non-cancerous tissue using qRT-PCR (n = 32). There was a significantly higher expressed miR-519a/522-5p in PDAC tissue compared with non-cancerous tissue ($P = 0.002$, Fig. 2A). Then we correlated the tumor miR-519a/522-5p level with matched serum exo-miR-519a/522-5p level and found a significant negative correlation ($P < 0.001$, Fig. 2B).

To assess the exosome transportation of miR-519a/522-5p in PDAC cells, we examined the expression of miR-519a/522-5p in various PDAC cell lines (PANC-1, BxPC-3, MIA PaCa-2, AsPC-1 and CFPAC-1), pancreatic epithelioid cells (CCC-HPE-2) and the extracellular exosomes in the culture medium. Compared to pancreatic epithelioid cells, PDAC cells displayed significantly increased cellular miR-519a/522-5p expression (Fig. 2C) and decreased medium miR-519a/522-5p level (Fig. 2D). There was a negative correlation between cellular and medium miR-519a/522-5p levels (Fig. 2E). In addition, we compared the miR-519a/522-5p levels between PDAC cells with different malignant behaviors, based on the current understanding of the characteristics of PDAC cell lines . PDAC cell lines with high metastatic activity (AsPC-1 and CFPAC-1) presented higher cellular miR-519a/522-5p expression and lower medium miR-519a/522-5p level than those with low metastatic activity (PANC-1, MIA PaCa-2 and BxPC-3) [15]. However, PDAC cell lines with different differentiation and proliferation exhibited no prominent difference (Fig. 2F) [16].

miR-519a/522-5p promotes invasiveness/metastasis of PDAC *in vitro* and *in vivo*

MiRNA mimics and inhibitors were used to evaluate the function of miR-519a/522-5p in PDAC cell lines (BxPC-3 and PANC-1), the transfection efficiency was assessed by qRT-PCR (Fig. S2A). There was no statistical significance in the relative cell survival and apoptotic rates between miR-519a/522-5p mimics/inhibitors group and the respective control group (Fig. S2B-C). In contrast, the invasion rate of the miR-519a/522-5p mimics group were significantly higher than that of the control group, whereas the miR-519a/522-5p inhibitors-transfected cells showed opposite result (Fig. 3A).

Subsequently, we constructed a stable miR-519a/522-5p-overexpressing PANC-1 cells (Fig. S2D), and established an orthotopic PDAC model in nude mice. Six weeks later, luciferase imaging system was applied to evaluate the metastasis of tumors and then the mice were sacrificed and autopsied (Fig. S2E). Compared with the control group, the overexpression of miR-519a/522-5p induced more liver metastasis (5/7 vs.1/7) (Fig. 3B-D). The further H&E and immunohistochemical analysis showed the overexpression of miR-519a/522-5p induced nodular metastatic foci in the liver (Fig. 3E).

miR-519a/522-5p could be transferred among PDAC cells via exosomes and promote invasiveness of recipient cells

To further investigate the extracellular transportation of exo-miRNA, we co-cultured untreated PANC-1 cells with the PANC-1 cells that transiently transfected with the Cy3-tagged miR-519a/522-5p for 48h. The fluorescently labeled miR-519a/522-5p was observed in the untreated PANC-1 cells through confocal microscopy. Moreover, when we added exosomes inhibitor (GW4869) into the co-culture system, the fluorescently labeled miR-519a/522-5p in the untreated PANC-1 cells was sharply weakened (Fig. 4A).

We next isolated exosomes from the serum-free medium of miR-519a/522-5p mimics, inhibitors, and control groups for further investigating whether exo-miR-519a/522-5p promotes invasiveness of recipient cells. The expression of exo-miR-519a/522-5p was assessed by qRT-PCR (Fig. S3A). The purified exosomes were co-cultured with untreated PANC-1 cells in transwell chamber for 48h. Compared with the control, increased cell invasion was observed when exo-miR-519a/522-5p mimics incubated with PANC-1 cells. In contrast, significant repression of cell invasion was found in PANC-1 cells co-cultured with exo-miR-519a/522-5p inhibitors (Fig. 4B). The uptake of exo-miR-519a/522-5p by PANC-1 cells was verified by qRT-PCR (Fig. S3B).

To improve the transfection efficiency, miR-519a/522-5p mimics were encapsulated into PANC-1-derived exosomes via electroporation. The encapsulation efficiency was approximately 20%. The transfection efficiency was greatly improved as compared to transient transfection and heavily miR-519a/522-5p loaded exosomes (elet-exo-miR-519a/522-5p) were obtained (Fig. S3C). The elet-exo-miR-519a/522-5p were co-cultured with untreated PANC-1 cells in transwell chamber for 48h. The uptake of elet-exo-miR-519a/522-5p by PANC-1 cells was verified by qRT-PCR and confocal microscopy (Fig. S3D-E). Compared with the control, the PANC-1 cells co-cultured with elect-exo-miR-519a/522-5p showed much stronger invasive potential (Fig. 4C).

miR-519a/522-5p-associated transcriptomics and metabolomics profiles in PDAC cells

We compared the differential transcriptome profiles between PANC-1 cells and stable PANC-1- miR-519a/522-5p cells (Fig. S4A). KEGG analysis revealed the significant enrichment of differential genes in cancer and metabolism pathways including proteoglycans in cancer, miRNAs in cancer, focal adhesion, adherents junction, central carbon metabolism in cancer and glycolysis/gluconeogenesis (Fig. S4B). The metabolomic analysis of the same specimens was performed to trace downstream variations of the transcriptomics. PCA plot (Fig. S4C) and PLS-DA plot (Fig. S4D) showed good sample segregation. The superclass distribution of metabolic features and differential metabolic features are shown in Fig. S4E-F. Mummichog analysis using MetaboAnalyst 4.0 showed that the metabolic features induced by miR-519a/522-5p overexpression were associated with arachidonic acid metabolism, amino sugar and nucleotide sugar metabolism, purine metabolism, 2-Oxocarboxylic acid metabolism, linoleic acid metabolism, galactose metabolism, fructose and mannose metabolism, pyrimidine metabolism, central carbon metabolism in cancer and glycolysis/gluconeogenesis metabolic pathways (Fig. S4G).

Cross-omics analysis reveals that miR-519a/522-5p drives glucose metabolic reprogramming in PDAC cells

We performed cross-omics analysis by simply overlapping the enriched pathways from metabolomics and transcriptomics and observed two common pathways as central carbon metabolism in cancer and glycolysis/gluconeogenesis. It may indicate a potential key role of glucose metabolism in miR-519a/522-5p-mediated molecules network.

Next, we calculated the differential abundance scores of metabolites and genes, which showed the tendency of them in certain pathway to be increased or decreased as compared to control group [17] (Fig. 5A). Among 53 metabolic pathways, 21 displayed increased levels of both genes and metabolites (right upper quadrant), indicating a consistency in metabolomics and transcriptomics data. Out of the 21 metabolic pathways, 8 were glycometabolism pathways including carbon metabolism, central carbon metabolism in cancer and glycolysis/gluconeogenesis. To concurrently visualize the regulation of both gene (right) and metabolite (left) levels in certain metabolic pathway, we performed Metabolograms analysis [17], which further proved the correlation between metabolomics and transcriptomics data (Fig. 5B).

The above analysis suggested an enhanced Warburg effect (i.e., increased glycolysis) after overexpression of miR-519a/522-5p in PDAC cells. Therefore, we further mapped the associated metabolites and genes to show the miR-519a/522-5p-induced metabolic reprogramming (Fig. 5C). Metabolites in glycolysis including G6P, F6P and PYR showed > 5-fold increase in abundance and genes encoding for the relevant enzymes including HK, PFK-1, ALDO, GAPDH, PGK, PGM, ENO, PKM and LDH were significantly increased. Genes encoding glucose and glutamine transporter (SLC2A1 and SLC1A5) were also significantly upregulated.

Further studies were conducted to validate whether miR-519a/522-5p could modulate glycolysis in PDAC cells. The ECAR increased as expected in both PANC-1 and BxPC-3 cells transfected with miR-519a/522-5p mimics (Fig. 5D), especially from 20 min to 60 min, which implied an elevated lactic acid formation during aerobic glycolysis.

miR-519a/522-5p directly targets SESN2 and promotes invasiveness of PDAC cells via enhancing Warburg effect

To further identify the specific pathways that directly targeted by miR-519a/522-5p, we firstly searched Targetscan (http://targetscan,org/), miRWalk (http://mirwalk.umm.uniheidelberg.de/) and miRDB (http://mirdb.org/miRDB/) databases. The potential target genes were overlapped with the down-regulated genes in our transcriptome dataset. The Venn diagram showed the overlap of 97 genes across the four gene sets (Fig. 6A). Then we integrated the glucose metabolic related gene sets from The Molecular Signatures Database (MSigDB, http://www.broadinstitute.org/gsea/msigdb) and three candidate genes were screened out (Fig. 6B). Western blotting and qRT-PCR results showed that overexpression of miR-519a/522-5p dramatically suppress SESN2 expression in PANC-1 cells (Fig. 6C-D), rather than ADIPOR2 and RNABP2 (Fig. S5A-B). Furthermore, the luciferase reporter assay indicated that overexpression of miR-519a/522-5p significantly inhibited luciferase activity in 293T cells expressing

wild type SESN2 reporters, whereas the mutant abolished this effect (Fig. 6E). The above data suggested that miR-519a/522-5p may target SESN2 directly.

Furthermore, we used lentivirus expressing Flag-SESN2 to upregulate SESN2 expression in both PANC-1 cells and stable PANC-1-miR-519a/522-5p cells. The transfection efficiency was demonstrated by Western blotting (Fig. S5C). Transwell and ECAR assay showed that overexpression of SESN2 could reverse the effects of miR-519a/522-5p induced high invasion and glycolysis in PANC-1 cells (Fig. 6F-G).

Discussion

In the present study, we proposed a novel serum biomarker panel including three exo-miRNAs (exo-miR-490-5p, exo-let-7g-3p and exo-miR-519a/522-5p), which proved to be excellent in the diagnosis of PDAC. Compared to the traditional tumor biomarkers such as CA19-9 and CEA, the panel not only significantly improved the diagnostic accuracy but also brought an indispensable supplement to CA19-9 negative PDAC patients.

Previous studies have proved the diagnostic role of serum exo-let-7a and exo-let-7b-5p in other types of cancer such as colorectal cancer and non–small cell lung cancer [18, 19]. In fact, Let-7 family (e.g., let-7b, let-7c, let-7i and let-7f) and miR-490-5p were found to be tumor suppressors. They were highly expressed in the serum but downregulated in tumor tissues in various cancer types [20–24]. Hypothesis has been defined that tumor cells might actively release tumor-suppressive miRNAs to facilitate their malignant characteristics. For example, Ohshima K et al. [25] showed that let-7 family was selectively secreted into the extracellular environment via exosomes in metastatic gastric cancer and proposed that the release of exo-let-7 was good for the maintenance of oncogenesis and cancer invasion. In consistent with previous studies, our result proved the diagnostic role of serum exo-let-7 and exo-miR-490-5p in PDAC.

In contrast, miR-519a/522-5p seemed to be an oncomiRNA that it was overexpressed in tumor tissues and associated with adverse patient outcome in breast cancer and hepatocellular carcinoma [26–28]. Consistent with previous studies, we found that miR-519a/522-5p was overexpressed in PDAC tissues as compared to para-tumor tissues. Moreover, *in vitro* and *in vivo* experiments demonstrated that miR-519a/522-5p could increase invasiveness and promote tumor metastasis of PDAC cells, which proved it as an oncomiRNA in PDAC. Interestingly, serum exo-miR-519a/522-5p was negatively correlated with tissue miR-519a/522-5p expression and played a pivotal role in both diagnosis and prognostic prediction of PDAC. It indicated that cancer cells might reluctantly loss the ‘tumor favorable’ oncomiRNA, which resulted in the unique expression pattern. The hypothesis could be proved by several previous studies in both PDAC and other types of cancer. For instance, the plasma level of exo-miR-19b, an oncomiRNA, was significantly lower in PDAC patients than that in control subjects [8]; low serum level of exo-miR-1226-3p was associated with tumor invasion or metastasis of PDAC [29]. In addition, low serum levels of exo-oncomiRNAs (e.g., miR-195-5p, miR-17-5p, miR-93-5p and miR-130a-3p) and high expression in tumor tissue were observed in patients with recurrent breast cancer [30]. Of note, we further proved that miR-

519a/522-5p could be efficiently transferred among PDAC cells via exosomes and dramatically increased the invasiveness of recipient cells, which further confirm the ‘tumor favorable’ oncomiRNA theory.

Although the oncogenic effect of miR-519a/522-5p has been proved in multiple cancer types, the molecular mechanism is still largely unknown. We previously demonstrated that the members of C19MC including miR-519a and miR-512 could co-target the downstream MAPK pathway and promote invasion in HCC [31, 32]. Tu et al. [27] found that miR-519a promoted colony formation, proliferation and cell cycle progression in HCC cell lines by targeting PTEN/PI3K/AKT signaling. Previous single-target analysis formulated target mRNA of miRNA according to the matched seed regions,, however, this method is unable to see the big picture and find key targets/pathways. A multi-omics study not only provides a highly efficient way to detect direct and indirect targets, but also presents a comprehensive molecular screening network to identify the core mechanisms [12].

Using a multi-omics strategy, we then constructed a comprehensive molecular network that was regulated by miR-519a/522-5p in PDAC cells and revealed a central role of glucose metabolic reprogramming in miR-519a/522-5p-drived oncogenic effect. We observed a series of genes (e.g., HK, PFK-1, ALDO, GAPDH, PGK, PGM, ENO, PKM and LDH) and metabolites (e.g., G6P, F6P and PYR) in the glycolysis pathway were significantly upregulated by miR-519a/522-5p. We further verified SESN2 as the target gene that was correlated with the glycolysis-associated molecular network. SESN2 is a member of stress-inducible protein and has been reported to play a critical role in the regulation of glucose metabolism and redox homeostasis via AMPK/mTOR/AKT axis [33, 34]. Overexpression of SESN2 could not only restrain mTORC1-S6K/AMPK activation [34, 35], but also upregulate the catalytic activity of mTORC2 and induce AKT phosphorylation [36], which ultimately limited cellular glycolysis. Interestingly, SESN2 was recently found as a tumor suppressor in colon cancer and lung cancer via p53/mTORC1 signaling [36, 37]. Taken together, we assumed that miR-519a/522-5p enhanced glycolysis in PDAC cells by directly targeting SESN2.

Although, the specificity and sensitivity of the unique serum exo-miRNA panel were demonstrated in our center, multi-center and large cohorts were needed to verify the diagnostic value of the panel. The cross-omics analysis offered fresh perspectives on the functional regulation of miRNAs. Using such technology, we demonstrated that miR-519a/522-5p exerted its metabolic reprogramming function by targeting SESN2. However, how the miR-519a/522-5p/SESN2 axis regulates Warburg effect in PDAC requires further in-depth experiments. Besides, we need to consider new strategies by targeting miR-519a/522-5p for the precise treatment of PDAC.

Conclusions

In summary, we demonstrated the diagnostic and prognostic effect of the serum exo-miRNAs in PDAC. We proposed a valid serum exo-miRNA panel with significant clinical value. From bedside to bench, we proved that the oncogenic effect of miR-519a/522-5p was achieved by targeting SESN2 and enhancing

the Warburg effect, and could be transported via exosomes between PDAC cells. Our study provided a novel insight into the precise diagnosis and treatment for PDAC.

Abbreviations

PDAC: Pancreatic ductal adenocarcinoma; miRNA: microRNA; exo-miRNAs: exosomal microRNAs; SESN2: sestrin2; AJCC: American Joint Committee on Cancer; TNM: tumor, node, metastasis; qRT-PCR: Quantitative Real-Time Reverse Transcription Polymerase Chain Reaction; CCK-8: Cell Counting Kit-8; LC-MS: liquid chromatographymass spectrometry; KEGG: Kyoto Encyclopedia of Genes and Genomes; ECAR: extracellular acidification rate; 2-DG: 2-deoxy-glucose; SD: standard deviation; ROC: Receiver operating characteristic curve; AUC: areas under the curve; CI: confidence interval; C19MC: chromosome 19 microRNA cluster; G6P: glucose 6-phosphate; F6P: fructose 6-phosphate; PYR: pyruvate; HK: hexokinase ; PFK-1: phosphofructokinase-1; ALDO: aldolase; GAPDH: glyceraldehyed 3-phosphate dehydrogenase; PGK: phosphoglycerate kinase; PGM: phosphoglycerate mutase; ENO: enolase; PKM: pyruvate kinase; LDH: lactate dehydrogenase; SLC2A1: solute carrier family 2 member 1; SLC1A5: solute carrier family 1 member 5

Declarations

Ethics approval and consent to participate

Written informed consent was obtained from all participants according to the guidelines of the Declaration of Helsinki. All the collection of specimens and animal handling in this work was reviewed and approved by the Medical Ethics Committee of The First Affiliated Hospital, Zhejiang University School of Medicine.

Consent for publication

All authors confrm their consent for publication the manuscript.

Availability of data and materials

The data generated in this study are not publicly available due to information that could compromise patient privacy or consent but are available upon reasonable request from the corresponding author.

Competing interests

The authors declare no potential conflicts of interest.

Funding

This study was supported by grants from the National Natural Science Foundation of China (82188102).

Authors’ contributions

TBL, QL, SF and RHC conceived the study and wrote the manuscript. TBL and QL provided funding support. SF, RHC, YML and JYJ collected and analyzed the clinical and pathological data. SF and RHC contributed to the analysis of clinical information. SF and RHC performed most of the experiments. HTH participated in bioinformatic analyses. QL, SF, RHC and HTH finished the statistical analysis. JLC performed H&E and immunohistochemistry staining. SF, RHC and QL finished the manuscript. TBL reviewed the manuscript. All authors have approved the final manuscript.

Acknowledgments

We would like to thank all colleagues in this work.

Author details

[1] Department of Pathology, The First Affiliated Hospital, Zhejiang University School of Medicine, Hangzhou, Zhejiang, China. [2] NHC Key Laboratory of Combined Multi-organ Transplantation, Hangzhou, Zhejiang, China. [3] Department of Hepatobiliary and Pancreatic Surgery, The First Affiliated Hospital, Zhejiang University School of Medicine, Hangzhou, Zhejiang, China. [4] Zhejiang Provincial Key Laboratory of Pancreatic Disease, The First Affiliated Hospital, Zhejiang University School of Medicine, Hangzhou, Zhejiang, China

References

1. Sung H, Ferlay J, Siegel RL, Laversanne M, Soerjomataram I, Jemal A, et al. Global Cancer Statistics 2020: GLOBOCAN Estimates of Incidence and Mortality Worldwide for 36 Cancers in 185 Countries. CA Cancer J Clin. 2021;71:209-49.
2. Mizrahi JD, Surana R, Valle JW, Shroff RT. Pancreatic cancer. Lancet. 2020;395:2008-20.
3. Schizas D, Charalampakis N, Kole C, Economopoulou P, Koustas E, Gkotsis E, et al. Immunotherapy for pancreatic cancer: A 2020 update. Cancer Treat Rev. 2020;86:102016.
4. Chan A, Prassas I, Dimitromanolakis A, Brand RE, Serra S, Diamandis EP, et al. Validation of biomarkers that complement CA19.9 in detecting early pancreatic cancer. Clin Cancer Res. 2014;20:5787-95.
5. Pegtel DM, Gould SJ. Exosomes. Annu Rev Biochem. 2019;88:487-514.
6. Yu D, Li Y, Wang M, Gu J, Xu W, Cai H, et al. Exosomes as a new frontier of cancer liquid biopsy. Mol Cancer. 2022;21:56.
7. Madhavan B, Yue S, Galli U, Rana S, Gross W, Müller M, et al. Combined evaluation of a panel of protein and miRNA serum-exosome biomarkers for pancreatic cancer diagnosis increases sensitivity and specificity. Int J Cancer. 2015;136:2616-27.
8. Wang L, Wu J, Ye N, Li F, Zhan H, Chen S, et al. Plasma-Derived Exosome MiR-19b Acts as a Diagnostic Marker for Pancreatic Cancer. Front Oncol. 2021;11:739111.

9. Takahasi K, Iinuma H, Wada K, Minezaki S, Kawamura S, Kainuma M, et al. Usefulness of exosome-encapsulated microRNA-451a as a minimally invasive biomarker for prediction of recurrence and prognosis in pancreatic ductal adenocarcinoma. J Hepatobiliary Pancreat Sci. 2018;25:155-61.
10. Wang X, Luo G, Zhang K, Cao J, Huang C, Jiang T, et al. Hypoxic Tumor-Derived Exosomal miR-301a Mediates M2 Macrophage Polarization via PTEN/PI3Kγ to Promote Pancreatic Cancer Metastasis. Cancer Res. 2018;78:4586-98.
11. Fu Y, Liu X, Chen Q, Liu T, Lu C, Yu J, et al. Downregulated miR-98-5p promotes PDAC proliferation and metastasis by reversely regulating MAP4K4. J Exp Clin Cancer Res. 2018;37:130.
12. Tao RA, Xzb C, Shi F, Hhb C, Szb C, Hxb C, et al. MiR-516a-3p is a Novel Mediator of Hepatocellular Carcinoma Oncogenic Activity and Cellular Metabolism. Engineering 2021. doi:https://doi.org/10.1016/j.eng.2021.07.020
13. Ling Q, Xu X, Wei X, Wang W, Zhou B, Wang B, et al. Oxymatrine induces human pancreatic cancer PANC-1 cells apoptosis via regulating expression of Bcl-2 and IAP families, and releasing of cytochrome c. J Exp Clin Cancer Res. 2011;30:66.
14. Zhang X, Ye P, Huang H, Wang B, Dong F, Ling Q. TCF7L2 rs290487 C allele aberrantly enhances hepatic gluconeogenesis through allele-specific changes in transcription and chromatin binding. Aging (Albany NY). 2020;12:13365-87.
15. Sipos B, Möser S, Kalthoff H, Török V, Löhr M, Klöppel G. A comprehensive characterization of pancreatic ductal carcinoma cell lines: towards the establishment of an in vitro research platform. Virchows Arch. 2003;442:444-52.
16. Monti P, Marchesi F, Reni M, Mercalli A, Sordi V, Zerbi A, et al. A comprehensive in vitro characterization of pancreatic ductal carcinoma cell line biological behavior and its correlation with the structural and genetic profile. Virchows Arch. 2004;445:236-47.
17. Hakimi AA, Reznik E, Lee CH, Creighton CJ, Brannon AR, Luna A, et al. An Integrated Metabolic Atlas of Clear Cell Renal Cell Carcinoma. Cancer Cell. 2016;29:104-16.
18. Ogata-Kawata H, Izumiya M, Kurioka D, Honma Y, Yamada Y, Furuta K, et al. Circulating exosomal microRNAs as biomarkers of colon cancer. PLoS One. 2014;9:e92921.
19. Jin X, Chen Y, Chen H, Fei S, Chen D, Cai X, et al. Evaluation of Tumor-Derived Exosomal miRNA as Potential Diagnostic Biomarkers for Early-Stage Non-Small Cell Lung Cancer Using Next-Generation Sequencing. Clin Cancer Res. 2017;23:5311-9.
20. Kou Y, Qiao L, Wang Q. Identification of core miRNA based on small RNA-seq and RNA-seq for colorectal cancer by bioinformatics. Tumour Biol. 2015;36:2249-55.
21. Hung CH, Hu TH, Lu SN, Kuo FY, Chen CH, Wang JH, et al. Circulating microRNAs as biomarkers for diagnosis of early hepatocellular carcinoma associated with hepatitis B virus. Int J Cancer. 2016;138:714-20.
22. Joosse SA, Müller V, Steinbach B, Pantel K, Schwarzenbach H. Circulating cell-free cancer-testis MAGE-A RNA, BORIS RNA, let-7b and miR-202 in the blood of patients with breast cancer and benign breast diseases. Br J Cancer. 2014;111:909-17.

23. Liu WJ, Xu Q, Sun LP, Dong QG, He CY, Yuan Y. Expression of serum let-7c, let-7i, and let-7f microRNA with its target gene, pepsinogen C, in gastric cancer and precancerous disease. Tumour Biol. 2015;36:3337-43.
24. Fang ZQ, Li MC, Zhang YQ, Liu XG. MiR-490-5p inhibits the metastasis of hepatocellular carcinoma by down-regulating E2F2 and ECT2. J Cell Biochem. 2018;119:8317-24.
25. Ohshima K, Inoue K, Fujiwara A, Hatakeyama K, Kanto K, Watanabe Y, et al. Let-7 microRNA family is selectively secreted into the extracellular environment via exosomes in a metastatic gastric cancer cell line. PLoS One. 2010;5:e13247.
26. Ward A, Shukla K, Balwierz A, Soons Z, König R, Sahin O, et al. MicroRNA-519a is a novel oncomir conferring tamoxifen resistance by targeting a network of tumour-suppressor genes in ER+ breast cancer. J Pathol. 2014;233:368-79.
27. Tu K, Liu Z, Yao B, Han S, Yang W. MicroRNA-519a promotes tumor growth by targeting PTEN/PI3K/AKT signaling in hepatocellular carcinoma. Int J Oncol. 2016;48:965-74.
28. Shi YH, Qi BB, Liu XB, Ding HM. Upregulation of miR-522 is associated with poor outcome of hepatocellular carcinoma. Eur Rev Med Pharmacol Sci. 2016;20:3194-8.
29. Wang C, Wang J, Cui W, Liu Y, Zhou H, Wang Y, et al. Serum Exosomal miRNA-1226 as Potential Biomarker of Pancreatic Ductal Adenocarcinoma. Onco Targets Ther. 2021;14:1441-51.
30. Sueta A, Yamamoto Y, Tomiguchi M, Takeshita T, Yamamoto-Ibusuki M, Iwase H. Differential expression of exosomal miRNAs between breast cancer patients with and without recurrence. Oncotarget. 2017;8:69934-44.
31. Rui T, Xu S, Zhang X, Huang H, Feng S, Zhan S, et al. The chromosome 19 microRNA cluster, regulated by promoter hypomethylation, is associated with tumour burden and poor prognosis in patients with hepatocellular carcinoma. J Cell Physiol. 2020;235:6103-12.
32. Rui T, Zhang X, Feng S, Huang H, Zhan S, Xie H, et al. The Similar Effects of miR-512-3p and miR-519a-2-5p on the Promotion of Hepatocellular Carcinoma: Different Tunes Sung With Equal Skill. Front Oncol. 2020;10:1244.
33. Budanov AV, Karin M. p53 target genes sestrin1 and sestrin2 connect genotoxic stress and mTOR signaling. Cell. 2008;134:451-60.
34. Lee JH, Budanov AV, Talukdar S, Park EJ, Park HL, Park HW, et al. Maintenance of metabolic homeostasis by Sestrin2 and Sestrin3. Cell Metab. 2012;16:311-21.
35. Sun X, Han F, Lu Q, Li X, Ren D, Zhang J, et al. Empagliflozin Ameliorates Obesity-Related Cardiac Dysfunction by Regulating Sestrin2-Mediated AMPK-mTOR Signaling and Redox Homeostasis in High-Fat Diet-Induced Obese Mice. Diabetes. 2020;69:1292-305.
36. Ro SH, Xue X, Ramakrishnan SK, Cho CS, Namkoong S, Jang I, et al. Tumor suppressive role of sestrin2 during colitis and colon carcinogenesis. Elife. 2016;5:e12204.
37. Sablina AA, Budanov AV, Ilyinskaya GV, Agapova LS, Kravchenko JE, Chumakov PM. The antioxidant function of the p53 tumor suppressor. Nat Med. 2005;11:1306-13.

Figures

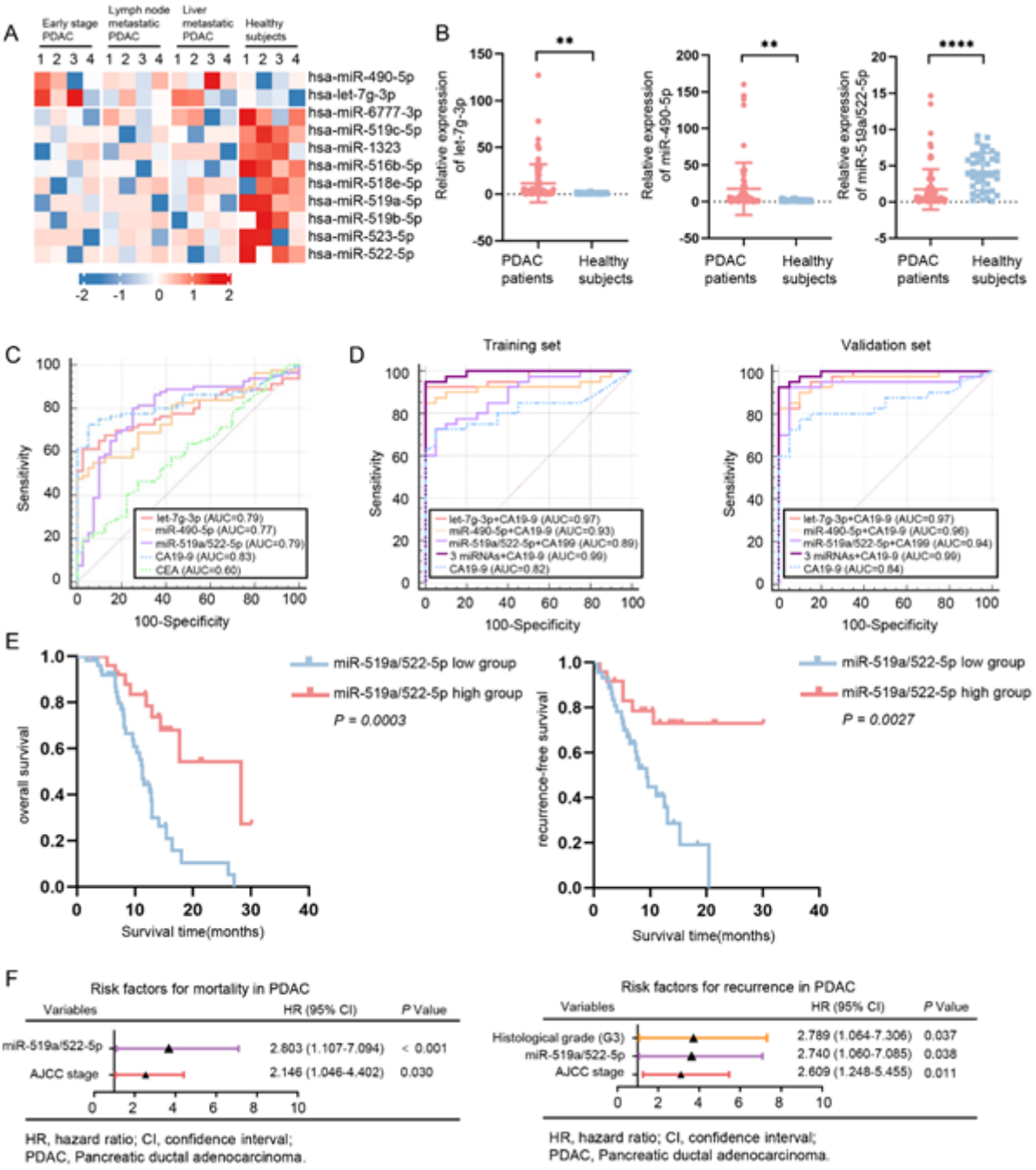

Figure 1

Serum exosomal miRNAs as biomarkers in PDAC. **A** Heatmap of the screened exo-miRNAs from serum of PDAC patients using a selection criteria of fold change > 2, $P < 0.05$ and the largest rank sum differences. **B** Relative expressions of serum exo-let-7g-3p, exo-miR-490-5p and exo-miR-519a/522-5p in 80 PDAC patients and 40 healthy subjects by qRT-PCR. **C** ROC curve analysis of 3 differential exo-miRNAs, CA19-9 and CEA. **D** ROC curve analysis of 3 differential exo-miRNAs combined CA19-9 in training set and validation set. **E** Prognostic impact of exo-miR-519a/522-5p on overall survival and recurrence -free

survival of PDAC patients via Kaplan–Meier curves. **F** The independent factor for tumor recurrence and patient death via multivariate survival analysis. (**P < 0.01, ****P < 0.0001)

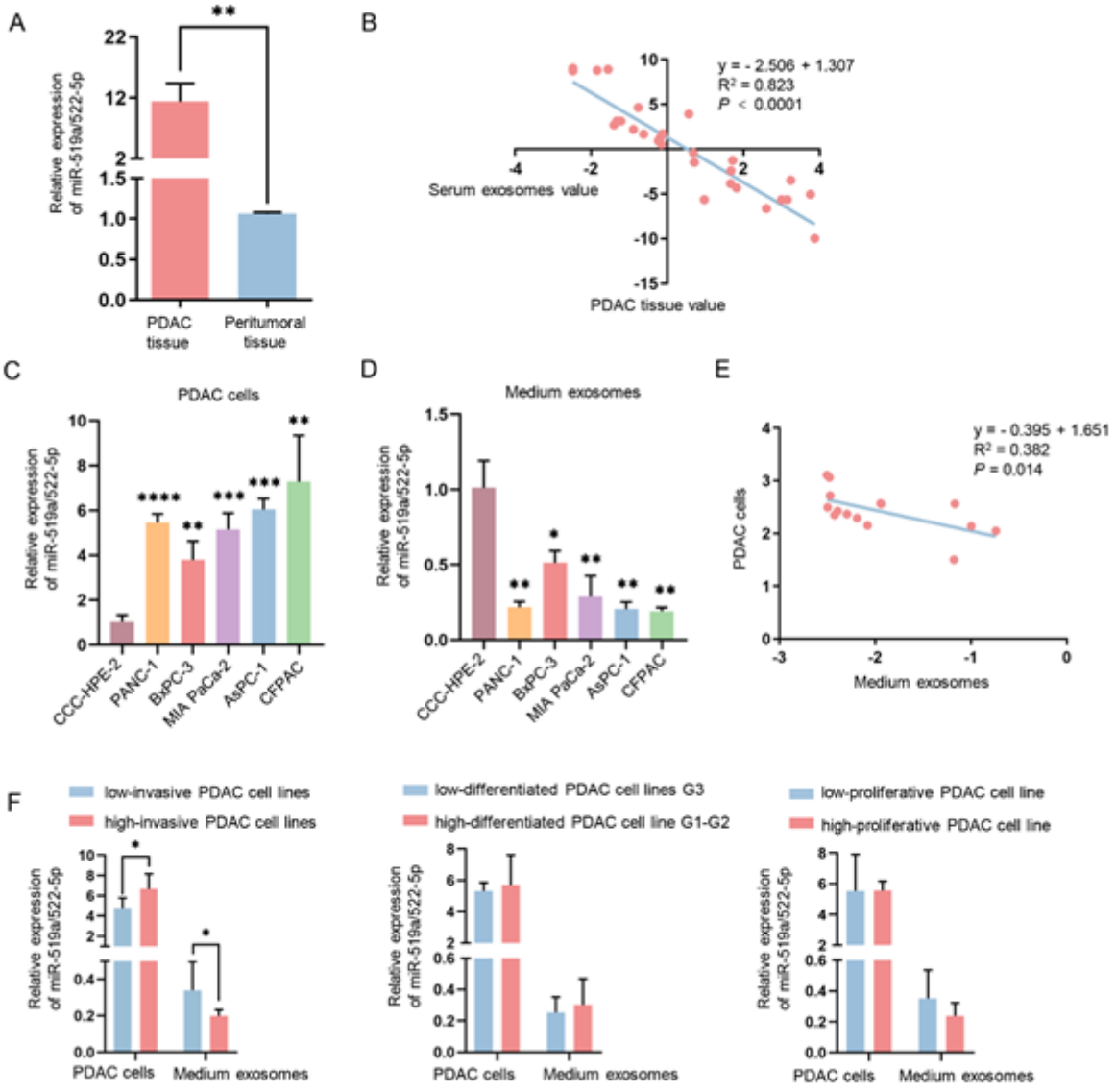

Figure 2

The expression of miR-519a/522-5p in PDAC tissue, cells and medium exosomes. **A** The relative expression of miR-519a/522-5p in PDAC tissue (n=32) and paired adjacent non-cancerous tissue (n=32) via qRT-PCR. **B** The correlation between the miR-519a/522-5p levels in PDAC tissue and matched serum exosomes. **C** and **D** The relative expression of miR-519a/522-5p in PDAC cells and their medium exosomes via qRT-PCR. **E** The correlation between the miR-519a/522-5p levels in PDAC cells and medium exosomes. **F** The relative expression of miR-519a/522-5p in PDAC cells with different malignant behaviors. (*P < 0.05, **P < 0.01, ***P < 0.001, ****P < 0.0001)

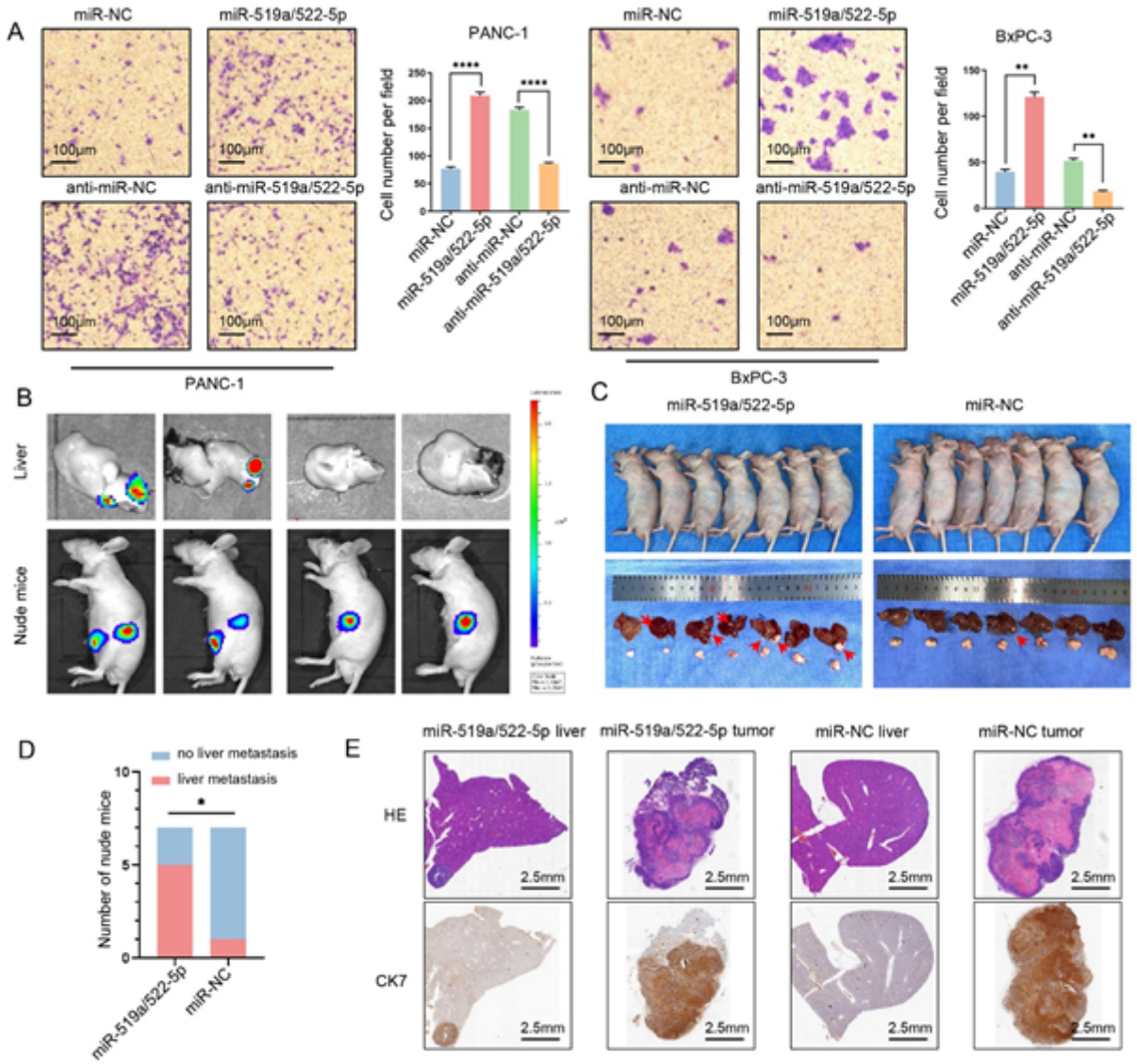

Figure 3

miR-519a/522-5p promotes invasiveness of PDAC *in vitro* and *in vivo.* **A** Transwell cell invasion assay of invasion rates in PANC-1 and BxPC-3 cells after transfection with miR-519a/522-5p mimics or inhibitor (Magnification, 100×). **B** The luciferase imaging of the orthotopic PDAC in nude mice model reflected the pancreas tumor burden and liver metastasis after being seeded with PANC-1 cells stably overexpressing miR-519a/522-5p or the controls. **C** and **D** The overexpression of miR-519a/522-5p induced more liver metastasis (5/7 vs.1/7) in nude mice via luciferase imaging system and autopsy. Red arrows indicate the hepatic metastasis foci. **E** The H&E and immunohistochemistry analysis of the orthotopic PDAC model in nude mice. (*$P < 0.05$, **$P < 0.01$, ****$P < 0.0001$)

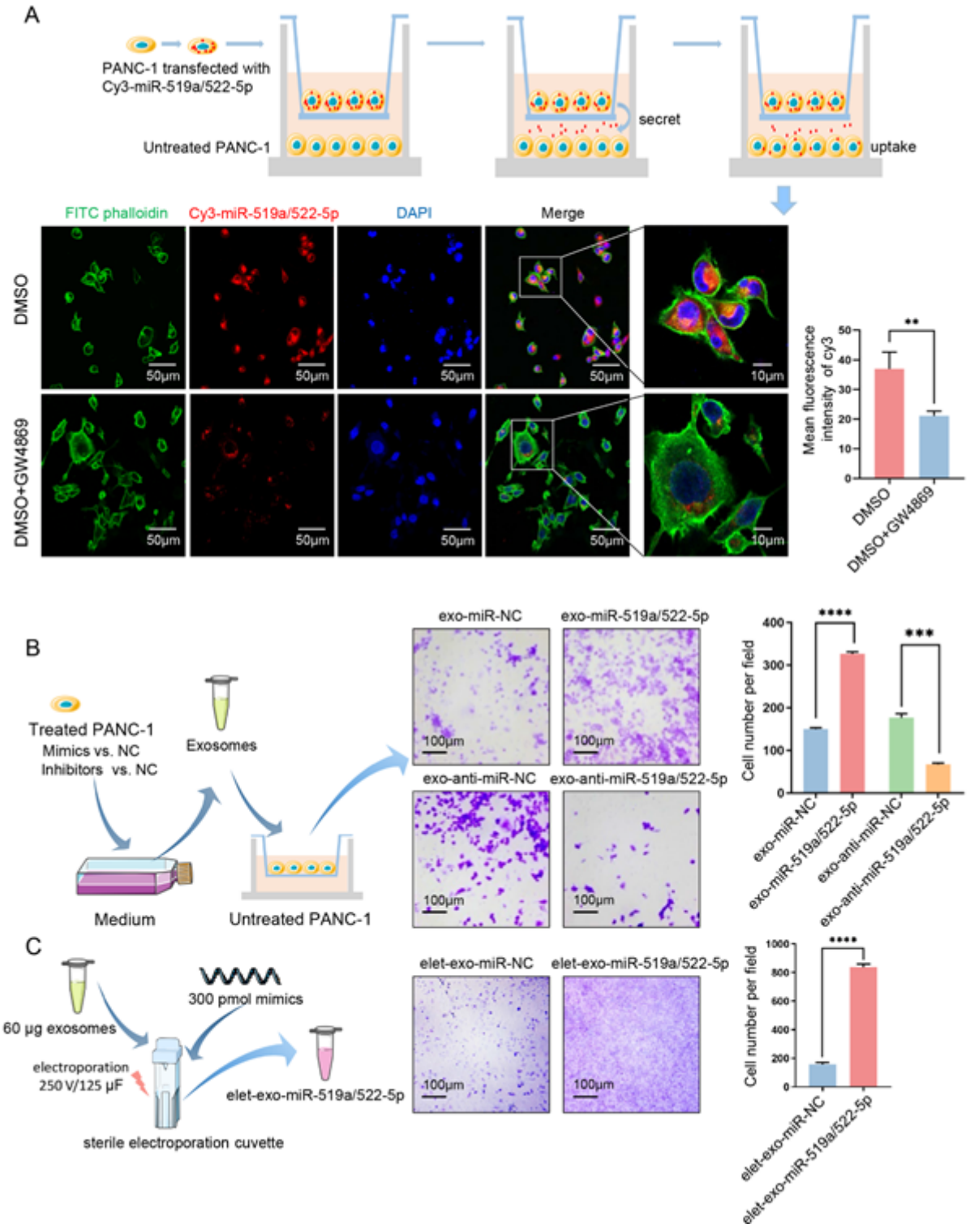

Figure 4

miR-519a/522-5p was transported between PDAC cells via exosomes and promotes invasiveness of recipient cells. **A** Cy3-tagged miR-519a/522-5p (the red fluorescence signal) was observed in the untreated PANC-1 cells via confocal microscopy. However, the red signal was significantly weakened when inhibitor of exosomes (GW4869) was added into the co-culture system (Magnification, 200× and 400×). **B** PANC-1 cells were transiently transfected with miR-519a/522-5p mimics or inhibitors. Exosomes were isolated and purified from the medium in each group.The purified exosomes were co-cultured with

untreated PANC-1 cells in transwell chamber for 48h. The invasion was increased when exo-miR-519a/522-5p mimics incubated with PANC-1 cells (Magnification, 100×). **C** Heavily miR-519a/522-5p loaded exosomes via electroporation also significantly promoted PANC-1 cells invasion. (***P* < 0.01, ****P* < 0.001, *****P* < 0.0001)

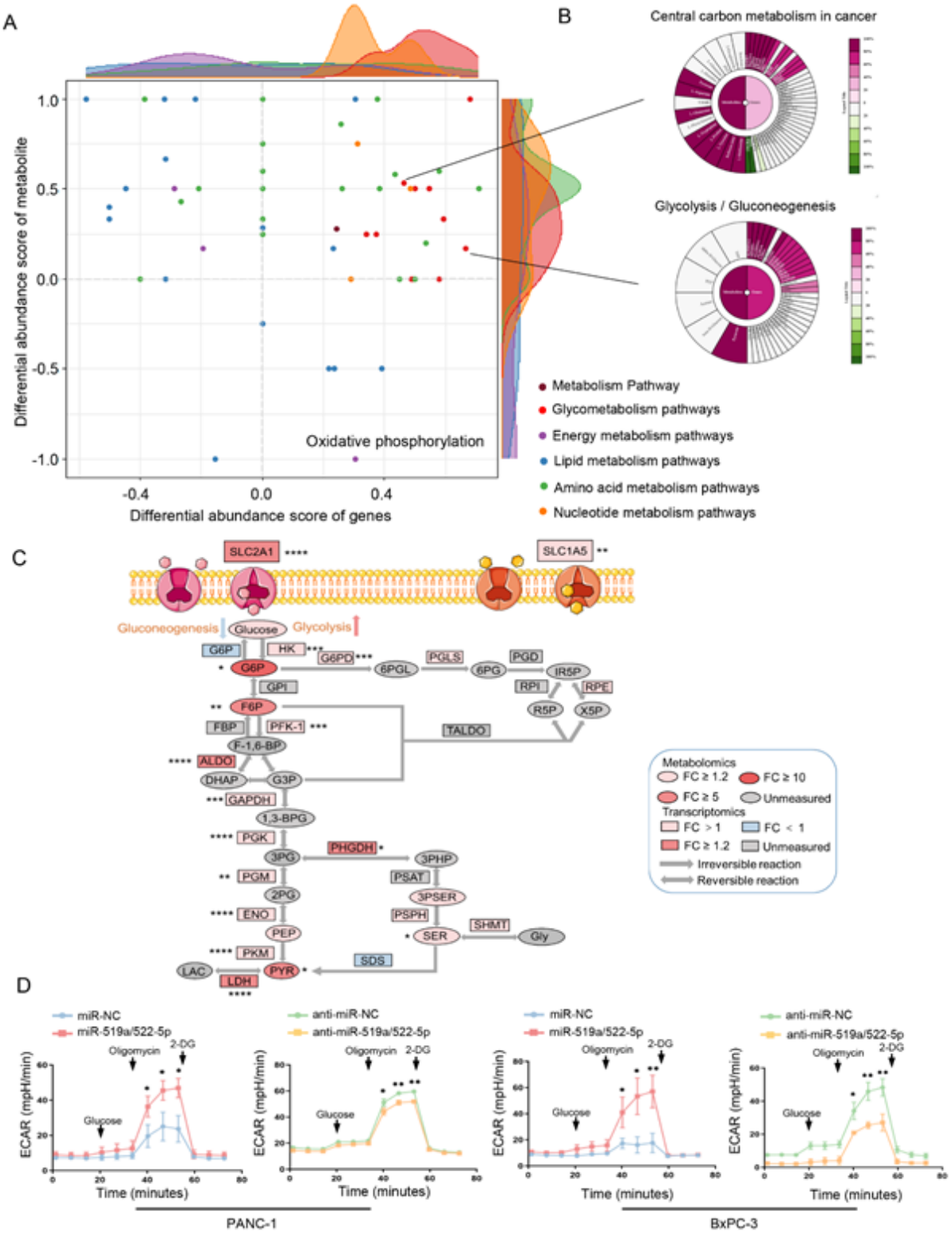

Figure 5

Cross-omics analysis between transcriptomics and metabolomics. **A** Differential abundance analysis shows the tendency of metabolites and genes in certain pathway. **B** Metabolograms analysis shows the correlation between metabolomics and transcriptomics data. **C** Glycolysis associated metabolites and genes map. **D** The overexpression of miR-519a/522-5p promoted glycolysis in both PANC-1 and BxPC-3 cells. (*$P < 0.05$, **$P < 0.01$, ***$P < 0.001$, ****$P < 0.0001$)

SLC2A1, solute carrier family 2 member 1; SLC1A5, solute carrier family 1 member 5; G6P, glucose 6-phosphate; F6P, fructose 6-phosphate; F-1,6-BP, fructose 1,6-bisphosphate; DHAP, dihydrxyacetone phosphate; G3P, glyceraldehyde 3-phosphate; 1,3BPG, 1,3-bisphosphoglycerate; 3PG, 3-phosphoglycerate; 2PG, 2-phosphoglycerate; PEP, phosphoenolpyruvate; PYR, pyruvate; LAC, lactate; 6PGL, 6-phosphogluconolactone; 6PG, 6-phosphpogluconate; R5P, ribulose 5-phosphate; X5P, xylulose 5-phosphate; 3PHP, 3-phosphohydroxypyruvate; 3PSER, 3-phosphoserine; SER, serine; GLY, glycine; HK, hexokinase; PFK-1, phosphofructokinase-1; ALDO, aldolase; GAPDH, glyceraldehyed 3-phosphate dehydrogenase; PGK, phosphoglycerate kinase; PGM, phosphoglycerate mutase; ENO, enolase; PKM, pyruvate kinase; LDH, lactate dehydrogenase; FC, fold change; 2-DG, 2-deoxy-glucose; GPI, phosphohexose isomerase; FBP, fructose-1,6-bisphosphatase; PGLS, 6-phosphogluconolactonase; PGD, 6-phosphogluconate dehydrogenase; TALDO, transaldolase.

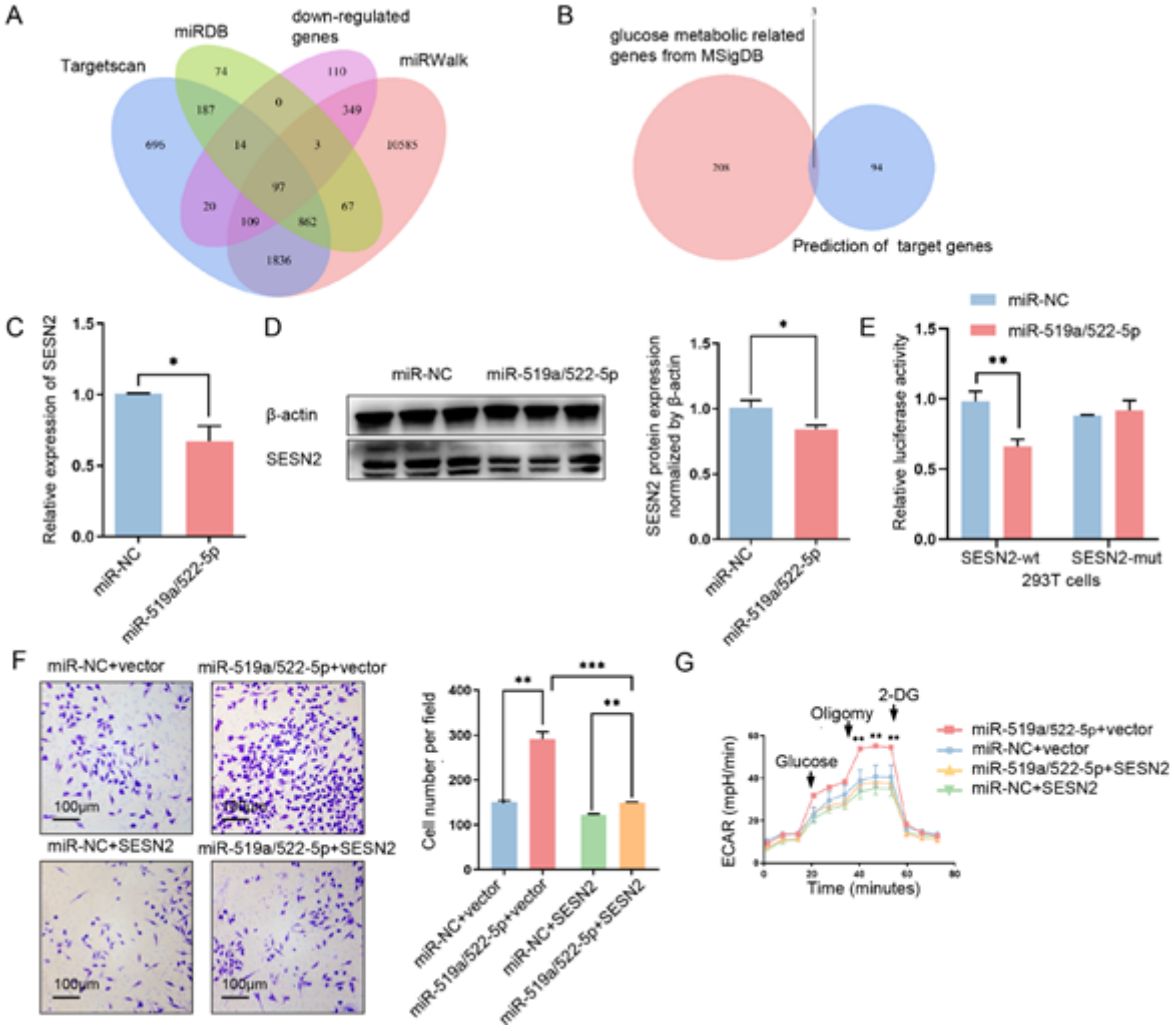

Figure 6

miR-519a/522-5p target SESN2 directly and promote invasion of PDAC cells via enhanced Warburg effect. **A** A Venn diagram was generated from Targetscan, miRWalk, miRDB databases and down-regulated genes in the transcriptome dataset. **B** A Venn diagram was generated from prediction of target genes and glucose metabolic related genes from MSigDB. **C** Expression of SESN2 in PANC-1 cells after transfection with miR-519a/522-5p was evaluated by qRT-PCR. **D** Expression of SESN2 protein in PANC-1 cells after transfection with miR-519a/522-5p was evaluated by western blotting. The grey value was measured using ImageJ software. **E** Relative SESN2 reporter activities in 293T cells cotransfected with miR-519a/522-5p and luciferase reporters. **F** Transwell cell invasion assay of invasion rates in PANC-1 cells after transfection with miR-519a/522-5p or miR-519a/522-5p+SESN(Magnification, 100×). G. ECAR assay in PANC-1 cells after transfection with miR-519a/522-5p or miR-519a/522-5p+SESN(vs. miR-519a/522-5p+SESN2). (*$P < 0.05$, **$P < 0.01$, ***$P < 0.001$)

Supplementary Files

This is a list of supplementary files associated with this preprint. Click to download.

- Additionalfile1.docx
- tableS6.xlsx